HHS Public Access

Author manuscript

Circ Heart Fail. Author manuscript; available in PMC 2019 August 01.

Published in final edited form as:

Circ Heart Fail. 2018 August ; 11(8): e004867. doi:10.1161/CIRCHEARTFAILURE.117.004867.

A Small Peptide Ac-SDKP Inhibits Radiation-Induced Cardiomyopathy

Umesh C. Sharma, MD, PhD[1], **Swati D. Sonkawade, PhD**[1], **Joseph A. Spernyak, PhD**[2], **Sandra Sexton, DVM**[3], **Juliane Nguyen, PhD**[4], **Suraj Dahal, MD**[1], **Kristopher M Attwood, PhD**[5], **Anurag K Singh, MD**[6], **Jop H. van Berlo, MD, PhD**[7], and **Saraswati Pokharel, MD, PhD**[8]

[1]Department of Medicine, Division of Advanced Cardiovascular Imaging in Cardiology, Jacob's School of Medicine and Biomedical Sciences, Buffalo, NY

[2]Preclinical Imaging Facility, Roswell Park Cancer Institute, Buffalo, NY

[3]Laboratory Animal Shared Resource Facility, Roswell Park Cancer Institute, Buffalo, NY

[4]Department of Pharmaceutical Sciences, School of Pharmacy, Buffalo, NY

[5]Department of Biostatistics and Bioinformatics, Roswell Park Cancer Institute, Buffalo, NY

[6]Department of Radiation Oncology, Roswell Park Cancer Institute, Buffalo, NY

[7]Lillehei Heart Institute, Department of Medicine, University of Minnesota, Minneapolis, MN

[8]Department of Pathology, Division of Thoracic Pathology and Oncology, Roswell Park Cancer Institute, Buffalo, NY

Abstract

Background—Advances in radiotherapy for thoracic cancers have resulted in improvement of survival. However, radiation exposure to the heart can induce cardiotoxicity. No therapy is currently available to inhibit these untoward effects. We examined whether a small tetrapeptide, N-acetyl-Ser-Asp-Lys-Pro (Ac-SDKP) can counteract radiation-induced cardiotoxicity by inhibiting macrophage-dependent inflammatory and fibrotic pathways.

Methods and Results—After characterizing a rat model of cardiac irradiation with MRI protocols, we examined the effects of Ac-SDKP in radiation-induced cardiomyopathy. We treated rats with Ac-SDKP for 18 weeks. We then compared myocardial contractile function and extracellular matrix by cardiac MRI, and the extent of inflammation, fibrosis and Mac-2 (galectin-3) release by tissue analyses. Since Mac-2 is a crucial macrophage-derived mediator of fibrosis, we performed studies to determine Mac-2 synthesis by macrophages in response to radiation, and change in pro-fibrotic responses by Mac-2 gene depleted cardiac fibroblasts after radiation. Cardiac irradiation diminished myocardial contractile velocities, and enhanced extracellular matrix deposition. This was accompanied by macrophage infiltration, fibrosis,

Address for Correspondence: Umesh Sharma, MD, PhD, Assistant Professor of Medicine, Clinical & Translational Research Center (Suite 7030), 875 Ellicott Street, Buffalo, New York 14203, Phone: 716.829.2663, Fax: 716.854.1840, sharmau@buffalo.edu.

Disclosures

None

cardiomyocyte apoptosis and cardiac Mac-2 expression. Ac-SDKP strongly inhibited these detrimental effects. Ac-SDKP migrated into the perinuclear cytoplasm of the macrophages and inhibited radiation-induced Mac-2 release. Cardiac fibroblasts lacking the Mac-2 gene showed reduced transforming growth factor β1 (TGF-β1), collagen I and collagen III expression after radiation exposure.

Conclusions—Our study identifies novel cardioprotective effects of Ac-SDKP in a model of cardiac irradiation. These protective effects are exerted by inhibiting inflammation, fibrosis, and reducing macrophage activation. This study shows a therapeutic potential of this endogenously released peptide to counteract radiation-induced cardiomyopathy.

Subject Codes

Inflammation; Fibrosis; Cardiomyopathy; Magnetic Resonance Imaging

Keywords

Ac-SDKP; Fibrosis; Macrophages; Mac-2; Radiotherapy

Despite early detection and state-of-the art therapeutic approaches for thoracic malignancies, development of radiation-induced cardiomyopathy can offset the promising benefits of radiotherapy. Currently, there are no specific therapeutic agents that are known to antagonize these effects. Radiation is the main trigger for the subsequent inflammation, fibrosis and cardiomyocyte loss leading to the development of myocardial dysfunction[1, 2]. A dose-dependent relation between radiation exposure and subsequent cardiac mortality was initially reported in a study cohort from Swedish Stockholm County[3]. Compared to non-irradiated patients, patients who had undergone chest radiotherapy had increased risk[4].

The existing therapy for radiation-induced cardiomyopathy is driven by conventional therapies developed for patients with other forms of cardiomyopathies. In recent years, there has been emphasis on exposing the patient to as little radiation as possible[5]. Despite these dose-limiting techniques, common cancers including breast, lungs and gastrointestinal cancers need significant radiation dose, and patients are at risk of developing both acute and long-term effects of radiation exposure to the heart.

In search of novel therapeutic agents, we assessed the therapeutic potential of a novel tetrapeptide, N-Acetyl-Ser-Asp-Lys-Pro (Ac-SDKP). Ac-SDKP was discovered by Lenfant *et al.* as a ubiquitous endogenous peptide[6]. The precursor of Ac-SDKP is thymosin-β4, which is essential for tissue healing and cell differentiation[6, 7]. Our previous studies in cardiac fibroblasts[8], as well as in two transgenic rat models of cardiac fibrosis have shown strong anti-fibrotic effects of Ac-SDKP [9–11]_ENREF_16. Ac-SDKP was also shown to have macrophage inhibitory effects in pre-clinical models[12]. In particular, Ac-SDKP was shown to inhibit the expression and activity of a carbohydrate-binding surface protein, Mac-2 (galectin-3) expressed by macrophages[9, 11]. We have previously shown an association between Mac-2 expression and cardiac fibrosis and heart failure in preclinical models and patients[13, 14].

Here we report a novel therapeutic approach to reduce the detrimental effects of radiation-induced cardiotoxicity. We have used a rat model of radiation-induced cardiomyopathy, which shows cardiomyocyte apoptosis, increased extracellular matrix, macrophage infiltration and Mac-2 expression. We also report that treatment with a small peptide, Ac-SDKP limits the fibro-inflammatory cascade triggered by radiation exposure, specifically involving macrophage activity. The results of this study demonstrate strong therapeutic promise, which can potentially benefit large number of cancer survivors.

Methods

The data that support the findings of this study are available from the corresponding author upon reasonable request.

Rat model of cardiac irradiation

We first optimized radiation dose using current dosimetry data obtained by radiation physicists at Roswell Park Cancer Institute (RPCI). Rats received experimental radiation with 250kV photons into the left hemithorax with a 1-cm cone and 2-mm thick lead plates to limit radiation exposure to the surrounding tissues. Anesthetized (isoflurane 4% induction, 2% maintenance) 10–12 week old male and female Sprague Dawley rats (Envigo) received a single dose of 30 Gray (Gy) radiation or Sham therapy into the left hemithorax using an orthovoltage radiator (Philips, Best, the Netherlands). Rats were observed during radiation exposure and for 30 minutes into recovery. The animal care and experimental protocols followed the US National Institutes of Health guidelines and were approved by the Institutional Animal Care and Use Committees of the RPCI at Buffalo, NY.

Ac-SDKP synthesis and delivery

Ac-SDKP was synthesized using Fmoc solid phase peptide synthesis (Genescript, Piscataway, NJ). Based on prior studies from our group[10] and others[15–17], we determined that a dose of 3.2 $mg.kg^{-1}.day^{-1}$ Ac-SDKP was required to reach maximal therapeutic effects. To continuously infuse Ac-SDKP at this rate, the purified peptide was delivered subcutaneously in a continuous manner by surgical implantation of Alzet® mini-osmotic pumps. All procedures were performed in sterile manner under anesthesia and analgesia was achieved with buprenorphine (0.05 $mg.kg^{-1}$ s.c.).

Ac-SDKP safety protocol—We first tested the clinical and hematological safety profile of Ac-SDKP in a smaller group of rats (N=5). These rats received identical doses of Ac-SDKP therapy for 4-weeks as other experimental groups. Complete blood count was performed at baseline and 1 month after radiation in rats with and without Ac-SDKP treatment. Rats were monitored daily for overall health and any skin irritation at the radiation site, and body weight was monitored bi-weekly.

Ac-SDKP therapy protocol—We used three experimental groups: (I) age-matched normal Sprague Dawley rats (N=12); (II) rats that received thoracic radiation (N=15); and (III) Ac-SDKP therapy group that received thoracic radiation followed by 18 weeks of subcutaneous Ac-SDKP (3.2 $mg.kg^{-1}.day^{-1}$) infusion (therapy initiated within 24 hours of

IR exposure). To minimize discomfort, all interventions were performed on anesthetized animals. Euthanasia procedure conformed to the guidelines from the Panel on Euthanasia of the American Veterinary Medical Association.

Cardiac magnetic resonance imaging

We used 4.7 Tesla preclinical magnetic resonance imaging (MRI) scanner using a 72 mm ID, quadrature transceiver coil and the ParaVision 3.0.2 acquisition platform (Bruker Biospin, Billerica, MA). Rats were anesthetized and maintained with 2–2.5% isoflurane during the duration of the imaging session. Body temperature and vital signs were maintained with an MR-compatible gating and monitoring system (Model 1025, SA Instruments, Stony Brook, NY). A detailed explanation for the MRI measurements of cardiac volumes, function, velocities and dynamic contrast imaging has been outlined in the supplemental data.

Immunohistochemistry and tissue morphometry

Macrophages were stained using a rat-specific anti-CD68 antibody (Abcam, Cambridge, MA; Ab-31630). The immunohistochemical studies were performed at the RPCI pathology resource core-lab. Considering the patchy distribution of inflammation, images were obtained from the pericardial half of each section that included an average of ten images from alternate microscopic field in a clock-wise fashion to cover the larger representative area of the myocardium. Mononuclear inflammatory cells with cytoplasmic staining were counted. The extent of myocardial fibrosis was visualized by trichrome staining. For a systematic image acquisition, the total myocardial area and the area of positive staining for flbrosis were quantified using NIH imaging software (National Institute of Health, Bethesda, MD, USA)[18].

TUNEL staining for apoptosis detection

TUNEL assay was performed using S7101 ApopTag® Plus Peroxidase in Situ Apoptosis Kit (Millipore Sigma, Burlington, MA). Briefly, 4μm formalin-fixed paraffin sections were treated with 0.3% hydrogen peroxide for 10 minutes. After digestion with 20 μg/ml proteinase-K for 17 minutes, slides were incubated with Terminal Deoxynucleotidyl Transferase (TdT) enzyme for 75 minutes. Following stepwise anti-digoxigenin-peroxidase and DAB chromogen (Dako, Santa Clara, CA; K3468) treatment, slides were counterstained with Hematoxylin and examined under the microscope. Pyknotic myocyte nuclei with homogenous brown nuclear staining were counted in average of ten randomly acquired images per tissue section as described above. The investigator was blinded to the experimental group during image acquisition and analyses.

Cardiomyocyte nuclear density

Myocyte nuclear density was assessed in the transverse sections of the trichrome-stained sections, using a cell quantification protocol reported previously[19].

Cell imaging studies

To examine the uptake of Ac-SDKP into the macrophages, we first performed *in vitro* cell imaging studies using Ac-SDKP-fluorescein isothiocyanate (FITC) agent.

Fluorophore-conjugated Ac-SDKP and scrambled peptide (Ac-KDPS) synthesis—The FITC-conjugated Ac-SDKP was synthesized using Fmoc solid phase peptide synthesis (Genescript, Piscataway, NJ) and FITC-conjugated Ac-KDPS was synthesized using similar Fmoc synthesis protocol (Lifetein, Somerset, NJ).

Ac-SDKP cytochemistry, confocal microscopy and FACS analysis—For these studies, cultured macrophages (RAW 264.7 cells, ATCC) were incubated with FITC-labeled Ac-SDKP or scrambled peptides (0.05, 0.1, 0.2 & 0.5μM). For uptake studies, cells were detached and analyzed with a BD LSR Fortessa flow cytometer. For peptide localization assays, cells were cultured on sterile cover slips, fixed with 4% PFA, mounted and imaged using a confocal microscope (ZEISS LSM 800 Laser scanning microscope) at 6300× magnification.

Enzyme-linked immunosorbent assays

Cellular Mac-2 levels—We used an indirect cell-directed enzyme-linked immunosorbent assay (ELISA) for the determination of radiation-induced Mac-2 expression by cultured macrophages (RAW 264.7 cell lines), (LS-F2009, Lifespan Biosciences, Seattle, WA). Cultured macrophages were exposed to 9Gy of radiation using a specialized orthovoltage radiation chamber and incubated for 24 hours. Subsequent Mac-2 expression by these cells was measured using anti-Mac-2 primary antibody per manufacturer's recommendations.

Myocardial Mac-2 levels—The myocardial Mac-2 protein levels were measured using rat-specific Horseradish peroxidase-dependent Mac-2 ELISA kit (ERLGALS3, Thermo Fisher Scientific, Waltham, MA). Myocardial tissue samples were homogenized in PBS, centrifuged and protein concentrations were measured. Standard curves were generated using the known concentration of recombinant Mac-2 protein. The Mac-2 concentration was quantified based on the optical densities measured at 490nm and normalized to tissue protein concentrations.

Cardiac fibroblast isolation and real-time PCR (RT-PCR) for collagen and TGF-β1 expression

To examine the effects of radiation on collagen synthesis, we isolated cardiac fibroblasts from 8–12 week-old Mac-$2^{+/+}$ and $Mac^{-/-}$ C57/BL6J mice (Jackson lab). We performed RT-PCR for collagen I, III and TGF-β1 expression after *in vitro* radiation exposure using the cardiac fibroblasts isolated from Mac-$2^{-/-}$ mice and wild-type controls (Mac-$2^{+/+}$). A detailed protocol for cell isolation, and RT-PCR and primer information has been outlined in the supplemental data.

Statistical Analyses

Quantitative endpoints were summarized by group using the mean and standard error of mean (SEM). When appropriate, the endpoints were modeled as a function of treatment

group (control, radiation alone, and radiation + Ac-SDKP) using one-way ANOVA models; with between-group comparisons made using Holm-Bonferroni adjusted post-hoc tests. Endpoint comparisons between Mac-$2^{+/+}$ and Mac-$2^{-/-}$ mice were made using unpaired t-tests. The association between cellular uptake and Ac-SDKP peptide concentration was evaluated using the Spearman correlation coefficient. All model/test assumptions were verified graphically using quantile-quantile and residual plots, with transformations applied as appropriate. All tests were two-sided at a nominal significance level of 0.05; that is, p-values <0.05 were considered significant.

Results

Changes in cardiac morphology and function quantified by cardiac MRI

We utilized newly developed MRI protocols to objectively assess cardiac function and extracellular matrix in our model.

Extracellular matrix volume—We compared the extracellular matrix by dynamic contrast imaging. Compared to baseline controls, radiation exposure led to delayed contrast clearance (reduced signal decay) and thus was consistent with increased myocardial extracellular matrix volume. Treatment with Ac-SDKP significantly improved the delayed contrast clearance dynamics as shown in Figure 1 (Panel A), which is consistent with less myocardial extracellular matrix (signal decay/min: control, −7.4±1.0; radiation, −4.7±0.7; and radiation + Ac-SDKP, −7.5±0.6, p=0.03 radiation *vs.* radiation + Ac-SDKP).

Left ventricular volume and function—Cardiac MRI with quantitative volumetric data analysis showed no significant differences in the LV ejection fraction (EF) or fractional shortening (FS). The stroke volumes and LV systolic and diastolic dimensions remained normal for all groups, with neither radiation exposure nor Ac-SDKP therapy showing significant changes (Supplemental Table 2).

Myocardial contractile/relaxation velocities—The baseline control rats had a mean Es of −2.5±0.4 cm/s and Ed of 3.5 ±0.6 cm/s. Rats with radiation exposure showed significantly reduced early systolic (contractile) and early diastolic (relaxation) velocities. Ac-SDKP therapy improved the radial contractility both during systole and diastole as shown in Figure 1 (Panel B and C).

Density and distribution of myocardial collagen tissue

We performed quantitative imaging of cardiac collagen content from Masson's trichrome-stained tissue sections. Radiation-exposure led to a patchy myocardial fibrosis more pronounced in the anterior wall. As shown in Figure 2, this increase in interstitial collagen was significantly inhibited by Ac-SDKP therapy (**% fibrosis**: control, 4.0±0.4; radiation, 9.3±0.8; radiation + Ac-SDKP, 4.9±0.8, p = 0.004 radiation *vs.* radiation + Ac-SDKP, N=8–10).

Presence of DNA degenerative changes and cardiomyocyte loss

Increased number of TUNEL positive cells were identified in rats after thoracic radiation exposure (control, 1.3±0.2, and radiation 4.4±0.4, p <0.001). Ac-SDKP therapy significantly decreased the number of TUNEL positive cells (1.9±0.4, p <0.001 *vs.* radiation) (Figure 3). Numerical density of cardiomyocytes nuclei was identified in each cross sectional image captured at high magnification. Connective tissue staining was subtracted from the total tissue area to determine the percentage that was represented by myocytes (% myocyte area). There was significant decrease in the nuclear density in radiation exposed rats compared to control (nuclei/HPF: control, 175±15, radiation, 116±5, p <0.001). Ac-SDKP therapy prevented the myocyte nuclear drop (145±6, p = 0.01 *vs.* radiation, N= 8–10/group) (Figure 4).

Examination of macrophage infiltration and activity

Myocardial macrophage density—We examined the degree of myocardial inflammation by counting the number of CD68 positive cells following chest radiation. We identified CD68 positive cells at myocardial interstitial spaces (with the exclusion of CD68-positive cells in the intravascular space). Control rats showed a small number of CD68 positive cells, likely representing resident tissue macrophages. As demonstrated in Figure 5, abundant CD68 positive cells were visualized in rats with radiation exposure, especially localized to the areas of patchy fibrotic changes. Ac-SDKP therapy significantly reduced CD68 cell infiltration to near-baseline levels (**cells/high power field**: control, 7±1; radiation, 24±5; radiation + Ac-SDKP, 11±1, p=0.008 radiation *vs.* radiation +Ac-SDKP, N=8–10).

Myocardial Mac-2 levels—We measured Mac-2 expression in the rat myocardium as a potential mediator of tissue fibrosis. Mac-2-specific ELISA on myocardial tissue homogenates showed a significant increase of Mac-2 levels after radiation exposure (Figure 6A). Ac-SDKP therapy significantly reduced the myocardial Mac-2 expression (control, 14±8; radiation, 85±15; radiation + Ac-SDKP, 36±9; p= 0.01 radiation *vs.* radiation + Ac-SDKP, N=8–10 per group).

Mac-2 release from the radiation-exposed macrophages—To determine the macrophage response to ionizing radiation and the effects of Ac-SDKP therapy, we measured Mac-2 levels in cultured macrophages with and without Ac-SDKP treatment. Macrophage-specific cell-cytokine ELISA was used to quantify radiation-induced Mac-2 expression. We found that exposure to 9 Gy radiation significantly increased the expression of Mac-2 protein by cultured macrophages within 24 hours, which was significantly inhibited by Ac-SDKP at 10μM (control, 1.5±0.1; radiation, 2.2±0.1; radiation + Ac-SDKP, 1.9 ± 0.1, p=0.01 radiation *vs.* radiation + Ac-SDKP, N=8 per group) (Figure 6B).

Ac-SDKP uptake by cultured macrophages

Confocal microscopy with 3D data processing demonstrated a robust uptake of FITC-Ac-SDKP into the cultured macrophages. The FITC-Ac-SDKP (0.5μM) was localized into the perinuclear region within 4 hours (Figure 7A, B and C). The FITC conjugated scrambled peptide used as control showed weak and diffuse intracellular staining (Figure 7D, E and F). Additionally, our FACS analysis to quantify the percentage of FITC-Ac-SDKP positive

macrophages showed dose-dependent uptake of FITC-Ac-SDKP by macrophages (R_S= 0.92; p<0.001) at the peptide concentration ranging from 0.05μM (10 ± 2%) to 0.5μM (33±1%) (Figure 7I). Compared to FITC-Ac-SDKP, the FITC-conjugated scrambled peptide was taken up by smaller percentage of cultured macrophages (Figure 7G and H).

Cardiac fibroblast response to radiation after Mac-2 gene deletion

To further investigate the pro-fibrotic effects of Mac-2 in radiation-induced cardiac fibrosis, we compared the radiation-induced pro-fibrotic response in cardiac fibroblasts isolated from Mac-$2^{-/-}$ mice and wild-type controls (Mac-$2^{+/+}$). Fibroblasts from control mice after radiation showed a robust increase of collagen I (WT, 16.0±4 vs. Mac-2 null, 1.0±1, p<0.001) collagen III (WT, 49.8±8 vs. Mac-2 null, 1.3±1, p<0.001) and TGFβ1 (WT, 7.3±1 vs. Mac-2 null, 1±1, p<0.001) gene expressions in 72 hours. Collagen I, Collagen III and TGFβ1 mRNA did not increase in Mac-$2^{-/-}$ fibroblasts in response to radiation (Figure 8A, 8B and 8C). The expression of TGFβ1 mRNA in the rat myocardium was measured in the heart specimens obtained at 18-weeks after radiation. We found no significant differences in the expression of cardiac TGFβ1 mRNA at the later stage (18-weeks) after radiation exposure (Figure 8D).

Safety profile of Ac-SDKP therapy

We performed initial *in vivo* study to examine the safety of Ac-SDKP in immune system. Importantly, there was no evidence of untoward effects, or any physical evidence of immune suppression following chest radiation with and without Ac-SDKP. There was a trend towards the reduction of lymphocyte count in radiated rats (P=NS), which was compensated by an increase in the number of monocytes (baseline 3.2±0.4%, radiation 4.2±0.2%, p =0.05). Although platelet counts were significantly decreased post-radiation (Supplemental Table 3), Ac-SDKP therapy did not change platelets, or white cell counts compared to the radiation group.

Discussion

Radiation-induced cardiomyopathy is a long-term side effect of radiotherapy of intrathoracic, chest wall and breast tumors when radiation field involves all or part of the heart[20]. There is a growing need for an effective and non-toxic pharmacologic agent that could counter these effects. Here, we identified a novel role for Ac-SDKP to inhibit the detrimental effects of radiation exposure to the heart. Previously, we have demonstrated that administration of Mac-2 directly into the heart causes myocardial fibrosis and loss of cardiac function[9, 13]. In this study, Ac-SDKP has shown anti-inflammatory, antifibrotic, cardiomyocye preserving and Mac-2 inhibitory effects in rat model of heart radiation. For the first time, we demonstrate that Ac-SDKP enters into the macrophages, and inhibits their activation and Mac-2 expression in response to radiation. Importantly, Mac-2 deletion abrogates radiation-induced collagen and TGF-β1 mRNA expression, highlighting an important role for Mac-2 in the pathogenesis of radiation-induced heart disease.

Radiation-Induced Cardiac Fibrosis: Virtuous Intentions, Malign Consequences?

Radiation-induced cardiac complications are related to total radiation dose, younger age at the exposure, a greater time elapsed since exposure, and concomitant use of cardiotoxic chemotherapeutic agents[21]. A seminal study by Kiscsatari and associates compared the effects of heart radiations at different doses. They demonstrated that cardiac radiation of 20–40Gy was well-tolerated and caused no animal death. A higher dose (50Gy) caused tachypnea, early cardiac functional decline, cardiac arrhythmias, and death[22]. We also examined the biological safety profile of 30Gy radiation in a subgroup of rats. We found that 30Gy of radiation did not cause acute clinical and hematological effects and all the animals survived on this dose. Therefore, balancing the acute morbid radiation toxicity and death *vs.* sub-acute or chronic cardiotoxicity, we used a radiation dose of 30Gy.

Radiation-related myocardial fibrosis can be initially asymptomatic often leading to late diagnosis[23]. Histologically, it is characterized by thick collagen bands criss-crossing the cardiac tissue, and separating and replacing cardiomyocytes[24]. Sridharan *et al* studied brown Norway rats exposed to local heart radiation, in which inflammation and fibrosis were seen at 3 and 6 months after radiation but most severe cardiac functional changes were seen 3 months after a single radiation dose of 24Gy[25]. The histomorphologic changes seen in our study are in agreement with the previously published data.

Prior Pre-Clinical Studies with Therapeutic Emphasis

Treatment of radiation-induced heart disease currently consists of standard medical therapy. Prior studies have examined the antifibrotic effects of an anti-oxidant agent Amifostine in rats[26]. However, Amifostine is not currently utilized due to its side effects. In 2013, Sridharan *et al* reported the effects of pentoxifylline and tocotrienols in a rat model of radiation-induced cardiac disease[27]. Pentoxifylline with and without tocotrienols did not alter increases in left ventricular diastolic pressure or deposition of collagen, although tocotreinols decreased left ventricular macrophage and mast cell densities. Since the effects of cardiac and pulmonary injury often co-exist after radiotherapy, ACE-inhibition was thought to be a promising therapeutic target, but the initial enthusiasm was offset by its side effects involving bradykinin accumulation which causes debilitating cough, angioedema and hypotension[28]. Clinically, it is difficult to discern whether the side effect of non-remitting cough is either due to bradykinin accumulation, cancer progression or pulmonary pathology. Based on its known mechanism of action, Ac-SDKP has no bradykinin-mediated side effects and also offers additional tissue healing and macrophages inhibitory effects, beyond the reported actions of ACE-inhibitors[29].

Cardiac MRI: One-Stop Shop under the Magnet

Majority of previous histological studies were performed in post-mortem specimens and cardiac function were characterized by conventional ultrasound technology. Recognizing the need for non-invasive imaging with superb spatial and temporal resolution and high reproducibly, we have utilized high-field cardiac MRI technique for myocardial morphological and functional assessments.

There are conflicting data in the literature regarding the effects of cardiac irradiation on overall global LV function. Studies have reported a wide array of results ranging from moderate reduction in ejection fraction, diastolic dysfunction, with some studies reporting supranormal LV contractility after radiation[21, 30, 31]. Recent developments in MRI imaging technology have enabled accurate evaluation of cardiac function as well as quantification of myocardial motion and deformation. While volumetric methods examine the global cardiac function, myocardial velocities can provide additional information at the pre-clinical level with quantification of initial force generation at onset of systole or diastole. The effects are determined by elasticity, fiber structure and myocardial geometry[32], which are expected to be affected by ionizing radiation.

Ac-SDKP: A Novel Therapeutic Target

In line with our prior observations in genetic models of ACE overexpression and other models of cardiac injury[11], we show strong anti-fibrotic and macrophage inhibitory effects of Ac-SDKP after localized heart radiation. In addition to these effects, we have, for the first time, demonstrated a cellular uptake of Ac-SDKP by cultured macrophages, which highlights the therapeutic relevance of this peptide after radiation exposure. The relevance of Ac-SDKP uptake around the nucleus can be reconciled to our prior observations that Ac-SDKP inhibited differentiation of bone marrow stem cells to macrophages and also inhibited macrophage migration, both effects that are likely mediated by proteins involved in nucleus-to-cytoplasmic shuttle, e.g., TGF-β, Smad2/3 and Mac-2 activity[10, 11]. Ac-SDKP was initially thought to play an important role as a “cytoprotective agent” by keeping the bone marrow stem cells at the quiescent state during chemotherapy[33, 34]. The anti-fibrotic effects can similarly be explained by a possible cell-cycle inhibitory effects of Ac-SDKP in cardiac fibroblasts. In fact, Kanasaki and associates reported the cyclin D1 inhibitory effects of Ac-SDKP[35]. Despite the robust macrophage inhibitory effects of Ac-SDKP, we have found no evidence of Ac-SDKP-induced immune suppression in our experimental model.

Increased Mac-2 Activity: A Newly Emerging Mechanism of Cardiac Fibrosis

Mac-2 (galectin-3) is a β-galactoside-binding lectin of ~30 kDa that has been implicated in inflammation and fibrosis[13, 36]. Identified first as an antigen on the surface of peritoneal macrophages, Mac-2 is the only chimera-type member of the galectin family[37]. Mac-2 plays a critical role in phagocytosis by macrophages when cross-linked by the Fcγ receptor[36]. Mac-2 is up-regulated when monocytes differentiate into macrophages[38]. As shown in our earlier study, Mac-2 is a specific and highly up-regulated marker of myocardial macrophages in failing hearts[13].

A recent study by Farrah and associates has shown reduced Mac-2 levels in response to Endothelin antagonism[39]. Increased Mac-2 expression has also been shown in a rat model of post-radiation pulmonary fibrosis[40]. Previous research has also demonstrated a causative role of Mac-2 in hepatic fibrosis[41]. Evidence for this new role of Mac-2 in radiation-induced cardiac fibrosis comes from our Mac-2 null fibroblast studies. Lack of expression of collagen I and III gene expression in Mac-2 null cardiac fibroblasts exposed to radiation suggests a crucial role of Mac-2 for radiation-induced fibrogenesis.

The antifibrotic and Mac-2 inhibitory effects of Ac-SDKP were examined by Liu et al in 2009, who reported that Ac-SDKP exerted anti-Mac-2 effects via the inhibition of Smad3 phosphorylation, which is an important transcription factor for collagen synthesis[9]. TGFβ plays a central role in organ fibrosis, particularly radiation-induced fibrosis. Previous studies have shown increase in TGFβ in the heart after radiation exposure. Prior studies reported an early increase of TGFβ mRNA following radiation, with no difference one month later[30, 42]. We have also found a robust increase of TGFβ mRNA expression in adult murine cardiac fibroblasts 72 hours after radiation-exposure, with no difference in the TGFβ expression in rat hearts 18 weeks after radiation. These data bring on an important concept of “hit and run” effects of ionizing radiation, in which initial “hit” triggers a fibro-inflammatory response and release of chronic mediators. In agreement, Kruse and associates also reported a peak increase of TGFβ mRNA at days 1 and 12 (maximum 6-fold of baseline), then returning to control levels by 1 month[42].

Conclusions and Therapeutic Implications

Although Ac-SDKP was found to have macrophage inhibitory and anti-fibrotic effects in some experimental models, there was a translational gap to transition these data into an effective therapy. To transition this peptide to the clinical arena, additional translational studies focused on the further evaluation of its pharmacodynamics and therapeutic efficacy will be required. However, we have provided the first direct evidence of cardio-protective effects of a novel endogenous peptide Ac-SDKP in radiation-induced cardiotoxicity.

Supplementary Material

Refer to Web version on PubMed Central for supplementary material.

Acknowledgments

We would like to acknowledge Steve Turowski for technical assistance during MRI scanning.

Sources of Funding

This research was supported by the National Center for Advancing Translational Sciences of the National Institutes of Health under award number UL1TR001412 to the University at Buffalo and Roswell Park Cancer Institute; and by Roswell Park and National Cancer Institute (NCI) under award number P30CA016056. Dr. Sharma is supported by Mentored Career Development Award from the NIH/NHLBI 1K08HL131987. Dr. Pokharel received support from Roswell Park Alliance Foundation (Award Number: 62-2609-01) and NIH/NHLBI Exploratory Research Grant (Award Number: 1R21 HL138555)

References

1. Chang HM, Okwuosa TM, Scarabelli T, Moudgil R, Yeh ETH. Cardiovascular Complications of Cancer Therapy: Best Practices in Diagnosis, Prevention, and Management: Part 2. J Am Coll Cardiol. 2017; 70:2552–2565. [PubMed: 29145955]
2. Chang HM, Moudgil R, Scarabelli T, Okwuosa TM, Yeh ETH. Cardiovascular Complications of Cancer Therapy: Best Practices in Diagnosis, Prevention, and Management: Part 1. J Am Coll Cardiol. 2017; 70:2536–2551. [PubMed: 29145954]
3. Gyenes G, Rutqvist LE, Liedberg A, Fornander T. Long-term cardiac morbidity and mortality in a randomized trial of pre- and postoperative radiation therapy versus surgery alone in primary breast cancer. Radiother Oncol. 1998; 48:185–90. [PubMed: 9783890]

4. Galper SL, Yu JB, Mauch PM, Strasser JF, Silver B, Lacasce A, Marcus KJ, Stevenson MA, Chen MH, Ng AK. Clinically significant cardiac disease in patients with Hodgkin lymphoma treated with mediastinal irradiation. Blood. 2011; 117:412–8. [PubMed: 20858859]
5. Armstrong GT, Liu Q, Yasui Y, Neglia JP, Leisenring W, Robison LL, Mertens AC. Late mortality among 5-year survivors of childhood cancer: a summary from the Childhood Cancer Survivor Study. J Clin Oncol. 2009; 27:2328–38. [PubMed: 19332714]
6. Lenfant M, Grillon C, Rieger KJ, Sotty D, Wdzieczak-Bakala J. Formation of acetyl-Ser-Asp-Lys-Pro, a new regulator of the hematopoietic system, through enzymatic processing of thymosin beta 4. Ann N Y Acad Sci. 1991; 628:115–25. [PubMed: 2069292]
7. Smart N, Risebro CA, Melville AA, Moses K, Schwartz RJ, Chien KR, Riley PR. Thymosin beta4 induces adult epicardial progenitor mobilization and neovascularization. Nature. 2007; 445:177–82. [PubMed: 17108969]
8. Pokharel S, Rasoul S, Roks AJ, van Leeuwen RE, van Luyn MJ, Deelman LE, Smits JF, Carretero O, van Gilst WH, Pinto YM. N-acetyl-Ser-Asp-Lys-Pro inhibits phosphorylation of Smad2 in cardiac fibroblasts. Hypertension. 2002; 40:155–61. [PubMed: 12154106]
9. Liu YH, D'Ambrosio M, Liao TD, Peng H, Rhaleb NE, Sharma U, Andre S, Gabius HJ, Carretero OA. N-acetyl-seryl-aspartyl-lysyl-proline prevents cardiac remodeling and dysfunction induced by galectin-3, a mammalian adhesion/growth-regulatory lectin. Am J Physiol Heart Circ Physiol. 2009; 296:H404–12. [PubMed: 19098114]
10. Pokharel S, van Geel PP, Sharma UC, Cleutjens JP, Bohnemeier H, Tian XL, Schunkert H, Crijns HJ, Paul M, Pinto YM. Increased myocardial collagen content in transgenic rats overexpressing cardiac angiotensin-converting enzyme is related to enhanced breakdown of N-acetyl-Ser-Asp-Lys-Pro and increased phosphorylation of Smad2/3. Circulation. 2004; 110:3129–35. [PubMed: 15520311]
11. Sharma U, Rhaleb NE, Pokharel S, Harding P, Rasoul S, Peng H, Carretero OA. Novel anti-inflammatory mechanisms of N-Acetyl-Ser-Asp-Lys-Pro in hypertension-induced target organ damage. Am J Physiol Heart Circ Physiol. 2008; 294:H1226–32. [PubMed: 18178715]
12. Peng H, Carretero OA, Brigstock DR, Oja-Tebbe N, Rhaleb NE. Ac-SDKP reverses cardiac fibrosis in rats with renovascular hypertension. Hypertension. 2003; 42:1164–70. [PubMed: 14581293]
13. Sharma UC, Pokharel S, van Brakel TJ, van Berlo JH, Cleutjens JP, Schroen B, Andre S, Crijns HJ, Gabius HJ, Maessen J, Pinto YM. Galectin-3 marks activated macrophages in failure-prone hypertrophied hearts and contributes to cardiac dysfunction. Circulation. 2004; 110:3121–8. [PubMed: 15520318]
14. van Kimmenade RR, Januzzi JL Jr, Ellinor PT, Sharma UC, Bakker JA, Low AF, Martinez A, Crijns HJ, MacRae CA, Menheere PP, Pinto YM. Utility of amino-terminal pro-brain natriuretic peptide, galectin-3, and apelin for the evaluation of patients with acute heart failure. J Am Coll Cardiol. 2006; 48:1217–24. [PubMed: 16979009]
15. Worou ME, Liao TD, D'Ambrosio M, Nakagawa P, Janic B, Peterson EL, Rhaleb NE, Carretero OA. Renal protective effect of N-acetyl-seryl-aspartyl-lysyl-proline in dahl salt-sensitive rats. Hypertension. 2015; 66:816–22. [PubMed: 26324505]
16. Nakagawa P, Masjoan-Juncos JX, Basha H, Janic B, Worou ME, Liao TD, Romero CA, Peterson EL, Carretero OA. Effects of N-acetyl-seryl-asparyl-lysyl-proline on blood pressure, renal damage, and mortality in systemic lupus erythematosus. Physiol Rep. 2017; 5:e13084. [PubMed: 28126732]
17. Junot C, Nicolet L, Ezan E, Gonzales MF, Menard J, Azizi M. Effect of angiotensin-converting enzyme inhibition on plasma, urine, and tissue concentrations of hemoregulatory peptide acetyl-Ser-Asp-Lys-Pro in rats. J Pharmacol Exp Ther. 1999; 291:982–7. [PubMed: 10565814]
18. Kawai M, Hongo K, Komukai K, Morimoto S, Nagai M, Seki S, Taniguchi I, Mochizuki S, Yoshimura M. Telmisartan predominantly suppresses cardiac fibrosis, rather than hypertrophy, in renovascular hypertensive rats. Hypertens Res. 2009; 32:604–10. [PubMed: 19424279]
19. Suzuki G, Iyer V, Lee TC, Canty JM Jr. Autologous mesenchymal stem cells mobilize cKit+ and CD133+ bone marrow progenitor cells and improve regional function in hibernating myocardium. Circ Res. 2011; 109:1044–54. [PubMed: 21885831]

20. Boerma M. Experimental radiation-induced heart disease: past, present, and future. Radiat Res. 2012; 178:1–6. [PubMed: 22663150]
21. Tapio S. Pathology and biology of radiation-induced cardiac disease. J Radiat Res. 2016; 57:439–448. [PubMed: 27422929]
22. Kiscsatari L, Sarkozy M, Kovari B, Varga Z, Gomori K, Morvay N, Lepran I, Hegyesi H, Fabian G, Cserni B, Cserni G, Csont T, Kahan Z. High-dose Radiation Induced Heart Damage in a Rat Model. In Vivo. 2016; 30:623–31. [PubMed: 27566082]
23. Heidenreich PA, Hancock SL, Lee BK, Mariscal CS, Schnittger I. Asymptomatic cardiac disease following mediastinal irradiation. J Am Coll Cardiol. 2003; 42:743–9. [PubMed: 12932613]
24. Fajardo LF, Stewart JR. Experimental radiation-induced heart disease. I. Light microscopic studies. Am J Pathol. 1970; 59:299–316. [PubMed: 5443637]
25. Sridharan V, Tripathi P, Sharma SK, Moros EG, Corry PM, Lieblong BJ, Kaschina E, Unger T, Thone-Reineke C, Hauer-Jensen M, Boerma M. Cardiac inflammation after local irradiation is influenced by the kallikrein-kinin system. Cancer Res. 2012; 72:4984–92. [PubMed: 22865451]
26. Kruse JJ, Strootman EG, Wondergem J. Effects of amifostine on radiation-induced cardiac damage. Acta Oncol. 2003; 42:4–9. [PubMed: 12665324]
27. Sridharan V, Tripathi P, Sharma S, Corry PM, Moros EG, Singh A, Compadre CM, Hauer-Jensen M, Boerma M. Effects of late administration of pentoxifylline and tocotrienols in an image-guided rat model of localized heart irradiation. PLoS One. 2013; 8:e68762. [PubMed: 23894340]
28. van der Veen SJ, Ghobadi G, de Boer RA, Faber H, Cannon MV, Nagle PW, Brandenburg S, Langendijk JA, van Luijk P, Coppes RP. ACE inhibition attenuates radiation-induced cardiopulmonary damage. Radiother Oncol. 2015; 114:96–103. [PubMed: 25465731]
29. Kanasaki K, Nagai T, Nitta K, Kitada M, Koya D. N-acetyl-seryl-aspartyl-lysyl-proline: a valuable endogenous anti-fibrotic peptide for combating kidney fibrosis in diabetes. Front Pharmacol. 2014; 5:70. [PubMed: 24782774]
30. Boerma M, Roberto KA, Hauer-Jensen M. Prevention and treatment of functional and structural radiation injury in the rat heart by pentoxifylline and alpha-tocopherol. Int J Radiat Oncol Biol Phys. 2008; 72:170–7. [PubMed: 18632215]
31. Seemann I, Gabriels K, Visser NL, Hoving S, te Poele JA, Pol JF, Gijbels MJ, Janssen BJ, van Leeuwen FW, Daemen MJ, Heeneman S, Stewart FA. Irradiation induced modest changes in murine cardiac function despite progressive structural damage to the myocardium and microvasculature. Radiother Oncol. 2012; 103:143–50. [PubMed: 22112779]
32. Kimura E, Tabata T, Tanaka H, Harada K, Yamada H, Nomura M, Oki T, Ito S. Left ventricular geometry and myocardial contractility in patients with essential hypertension evaluated by myocardial velocity profile. J Am Soc Echocardiogr. 2005; 18:1222–9. [PubMed: 16275535]
33. Volkov L, Quere P, Coudert F, Comte L, Praloran V. The tetrapeptide AcSDKP, a physiological inhibitor of normal cell proliferation, reduces the S phase entry of continuous cell lines. Exp Cell Res. 1996; 223:112–6. [PubMed: 8635482]
34. Lombard MN, Sotty D, Wdzieczak-Bakala J, Lenfant M. In vivo effect of the tetrapeptide, N-acetyl-Ser-Asp-Lys-Pro, on the G1-S transition of rat hepatocytes. Cell Tissue Kinet. 1990; 23:99–103. [PubMed: 2317837]
35. Kanasaki K, Haneda M, Sugimoto T, Shibuya K, Isono M, Isshiki K, Araki S, Uzu T, Kashiwagi A, Koya D. N-acetyl-seryl-aspartyl-lysyl-proline inhibits DNA synthesis in human mesangial cells via up-regulation of cell cycle modulators. Biochem Biophys Res Commun. 2006; 342:758–65. [PubMed: 16497271]
36. Sano H, Hsu DK, Apgar JR, Yu L, Sharma BB, Kuwabara I, Izui S, Liu FT. Critical role of galectin-3 in phagocytosis by macrophages. J Clin Invest. 2003; 112:389–97. [PubMed: 12897206]
37. Cherayil BJ, Chaitovitz S, Wong C, Pillai S. Molecular cloning of a human macrophage lectin specific for galactose. Proc Natl Acad Sci U S A. 1990; 87:7324–8. [PubMed: 2402511]
38. Liu FT, Hsu DK, Zuberi RI, Kuwabara I, Chi EY, Henderson WR Jr. Expression and function of galectin-3, a beta-galactoside-binding lectin, in human monocytes and macrophages. Am J Pathol. 1995; 147:1016–28. [PubMed: 7573347]

39. Farrah TE, Anand A, Miller-Hodges E, Mills NL, Webb DJ, Dhaun N. Endothelin antagonism reduces circulating galectin-3 in patients with proteinuric chronic kidney disease. Kidney Int. 2018; 93:270. [PubMed: 29291821]

40. Kasper M, Hughes RC. Immunocytochemical evidence for a modulation of galectin 3 (Mac-2), a carbohydrate binding protein, in pulmonary fibrosis. J Pathol. 1996; 179:309–16. [PubMed: 8774488]

41. Henderson NC, Mackinnon AC, Farnworth SL, Poirier F, Russo FP, Iredale JP, Haslett C, Simpson KJ, Sethi T. Galectin-3 regulates myofibroblast activation and hepatic fibrosis. Proc Natl Acad Sci U S A. 2006; 103:5060–5. [PubMed: 16549783]

42. Kruse JJ, Bart CI, Visser A, Wondergem J. Changes in transforming growth factor-beta (TGF-beta 1), procollagen types I and II mRNA in the rat heart after irradiation. Int J Radiat Biol. 1999; 75:1429–36. [PubMed: 10597916]

WHAT IS NEW?

- The most common thoracic malignancies are treated with ionization radiation (IR). Since IR is responsible for early and delayed cardiac damage, there is an urgent need to identify novel therapeutic strategies to mitigate these effects.
- This article reports a preclinical study that examines the anti-inflammatory and anti-fibrotic effects of a small peptide, Ac-SDKP in a rodent model of thoracic IR exposure. Chronic Ac-SDKP infusion inhibits macrophage activity, reduces cardiac fibrosis and preserves myocardial contractile forces.

WHAT ARE THE CLINICAL IMPLICATIONS?

- We anticipate that this study will have important therapeutic implications to inhibit radiation-induced cardiotoxicity, thus benefitting a large cohort of thoracic cancer survivors treated with IR.
- In the future, the protective effects of Ac-SDKP can be extended to benefit larger groups, including survivors of non-thoracic cancers, in which post radiation morbidity remains very high.
- Since Ac-SDKP is an endogenous peptide, concerns for the potential peptide-related toxicities including immune-compromise are greatly reduced.

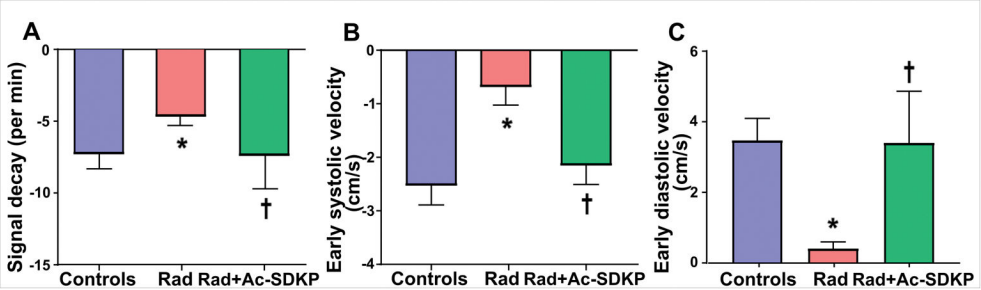

Figure 1. Bar diagrams comparing extracellular volume fraction and early cardiac contractile and relaxation velocities measured by cardiac MRI

Panel A: Post-contrast MR imaging to compare the Gadolinium signal decay (***rate of contrast clearance***), which strongly correlated with the extracellular matrix/fibrosis. Slower decreases in the signal (radiation group) indicates gadolinium is retained in the myocardial interstitial space as a result of radiation-induced extracellular matrix expansion. Ac-SDKP therapy normalized the decay curve. N = 10–15, *, P =0.03 radiation *vs.* control, †, P =0.03 radiation *vs.* radiation + Ac-SDKP. **Panel B:** represents bar diagrams comparing the Early-systolic (Es) radial velocities in the short-axis cine MRI images. The Es velocities (due to cardiomyocyte-shortening) are shown in the negative axis. Radiation exposure significantly reduced Es, which was inhibited by Ac-SDKP *, P =0.01 radiation *vs.* control, †, P =0.04 radiation *vs.* radiation + Ac-SDKP. **Panel C**: represents Early-diastolic (Ed) radial velocities in the short-axis cine MRI images. The Ed velocities (due to cardiomyocyte-lengthening) are shown in the positive axis (*panel D*). Radiation exposure led to significant reduction of Ed, which was improved by Ac-SDKP therapy *, P =0.02 radiation *vs.* control, †, P =0.03 radiation *vs.* radiation + Ac-SDKP.

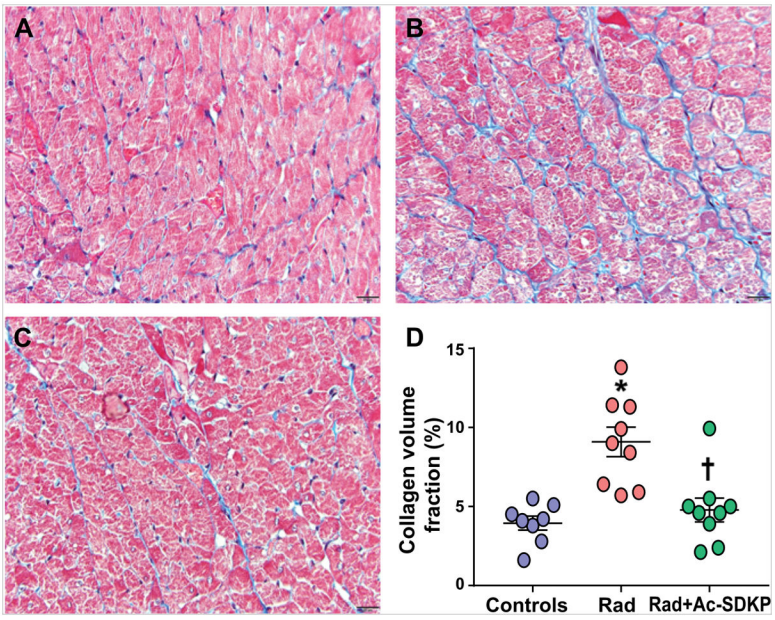

Figure 2. Comparison of interstitial collagen deposition in the myocardium

Panel A to **C** are the representative images of Masson's trichrome staining of rat myocardial sections. **Panel A**: Wild type control; **Panel B**: Radiation; and **Panel C**: Radiation + Ac-SDKP. Blue staining represents collagen. **Panel D**: Quantification of interstitial collagen volume fraction in control and radiation exposed rats with and without Ac-SDKP therapy. Magnification ×400. N = 8–10, *, P <0.001 radiation *vs.* control, †, P =0.004 radiation *vs.* radiation + Ac-SDKP.

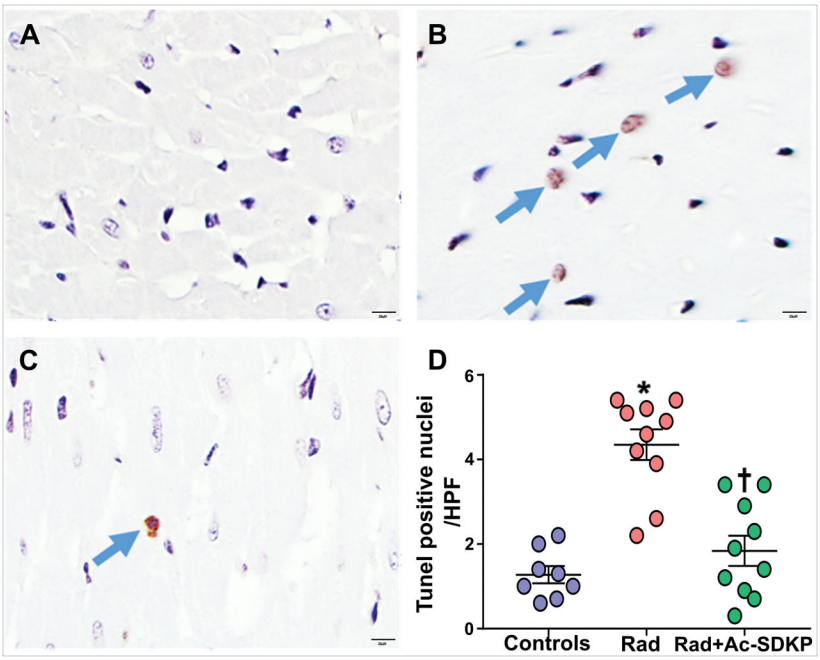

Figure 3. Analysis of cardiomyocyte DNA degradation by TUNEL staining of the myocardial sections

Panel A–C show representative images in control (A), radiation exposed (B) and radiation + Ac-SDKP treated groups. **Panel D:** Represents quantification of tunnel stained myocyte nuclei per high power field. Arrows highlight TdT positive (apoptotic) myocytes. Magnification ×400. N = 8–10, *, P <0.001 radiation vs. control, †, P <0.001 radiation *vs.* radiation + Ac-SDKP.

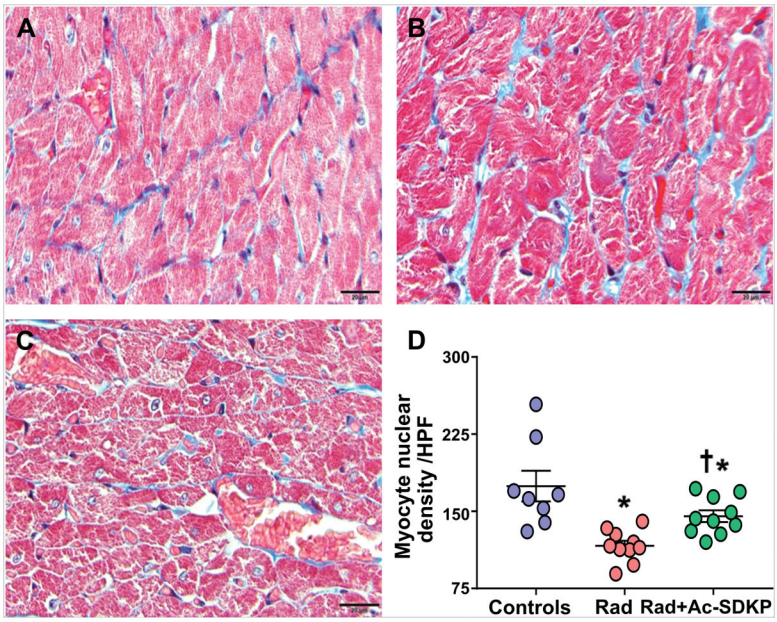

Figure 4. Comparison of myocyte nuclear density

Post-radiation, increased number of myocyte nuclear drop outs were seen, which was prevented by Ac-SDKP therapy. **Panel** A: Wild type control; **Panel B**: Radiation; **Panel C**: Radiation + Ac-SDKP; **Panel D**: Quantitative dot plots. Magnification ×400. N = 8–10, *, P<0.001 radiation *vs.* control, *, P =0.04 radiation + Ac-SDKP *vs.* control, †, P =0.01 radiation *vs.* radiation + Ac-SDKP.

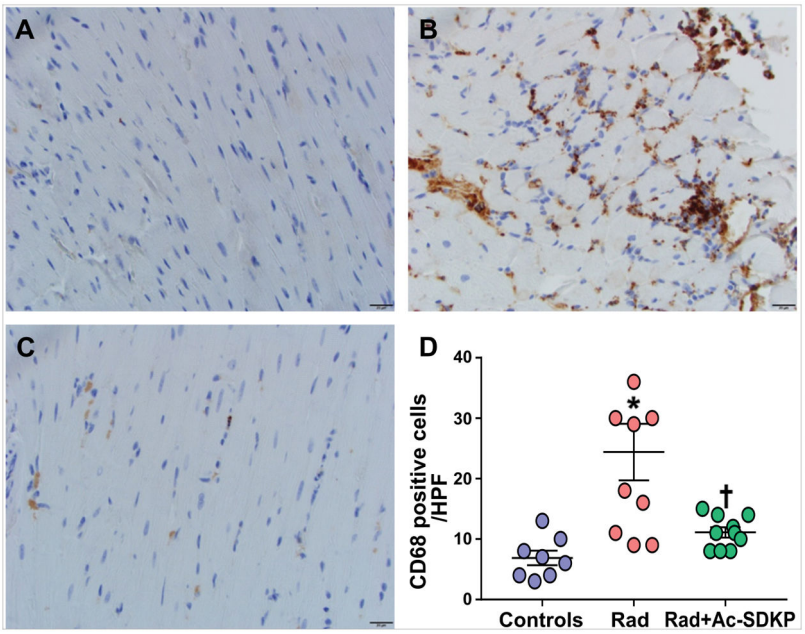

Figure 5. Assessment of myocardial macrophage infiltration

Panel A–C: Representative images of CD68-stained myocardial macrophages**. Panel A**: Wild type control; **Panel B**: Radiation; **Panel C**: Radiation + Ac-SDKP. Brown stained cells represent macrophages × 400. **Panel D**: Quantification of myocardial macrophages in control and radiation exposed rats with and without Ac-SDKP therapy. N = 8–10, *, P < 0.001 radiation *vs.* control, †, P =0.008 radiation *vs.* radiation + Ac-SDKP.

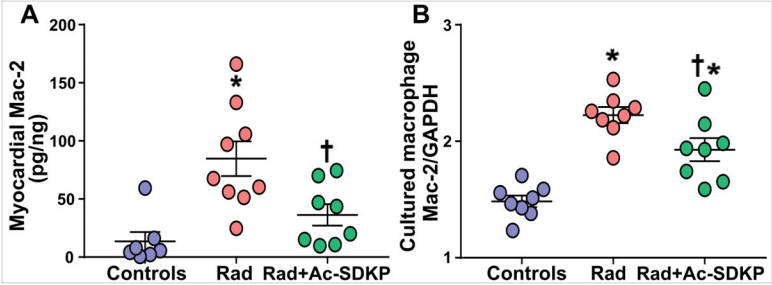

Figure 6. Mac-2 expression in myocardial tissue homogenate and cultured macrophages measured by ELISA

Panel A: Mac-2 levels in myocardial tissue homogenate. Radiation exposure significantly increased myocardial Mac-2 levels, which was inhibited by Ac-SDKP. N = 7–10, *, P =0.001 radiation *vs.* control, †, P =0.01 radiation *vs.* radiation + Ac-SDKP. **Panel B**: Mac-2 expression in cultured macrophages. Radiation exposure (9Gy) significantly increased Mac-2 expression, which was inhibited by Ac-SDKP (10μM). N = 8 per group, *, P =0.001, radiation *vs.* control; †, P=0.02, radiation *vs.* radiation + Ac-SDKP.

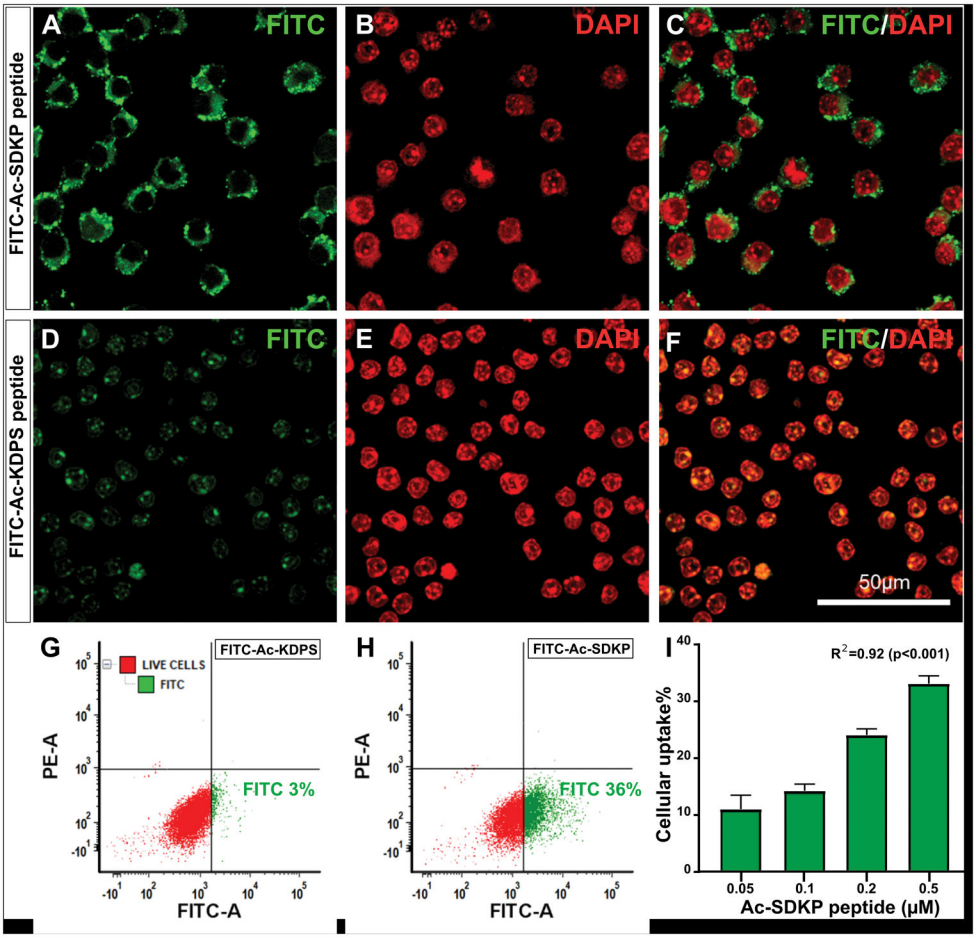

Figure 7. Confocal microscopy images showing the uptake and localization of FITC-Ac-SDKP conjugate into cultured macrophages

Macrophages were incubated with FITC labelled Ac-SDKP and scrambled peptide for 4 hours and the cells were prepared for immunofluorescence study. **A:** Representative confocal image showing FITC-labelled peptide (green) localized in to the perinuclear region; **B:** DAPI stained macrophage nuclei (red), and **C**: Merged FITC and DAPI images. **Panel D–F** shows non-specific diffuse and weak cytoplasmic staining of scrambled peptide, FITC-Ac-KDPS (FITC in green and DAPI in red). **Panel G–H** are representative fluorescence-activated cell sorting (FACS) results corresponding to scrambled peptide and FITC-Ac-SDKP probe, respectively. The gating was set to show FITC-A positive cell population in green and negative viable cells in red. **A–H** are representative results for macrophages incubated with Ac-SDKP at 0.5µM concentration. **Panel I**: Bar graph showing percentage of cells with FITC uptake at different concentration of Ac-SDKP with background subtraction of scrambled peptide by FACS analysis. N= 3, R^2 = 0.92 ($p < 0.001$). Scale bar:50µm.

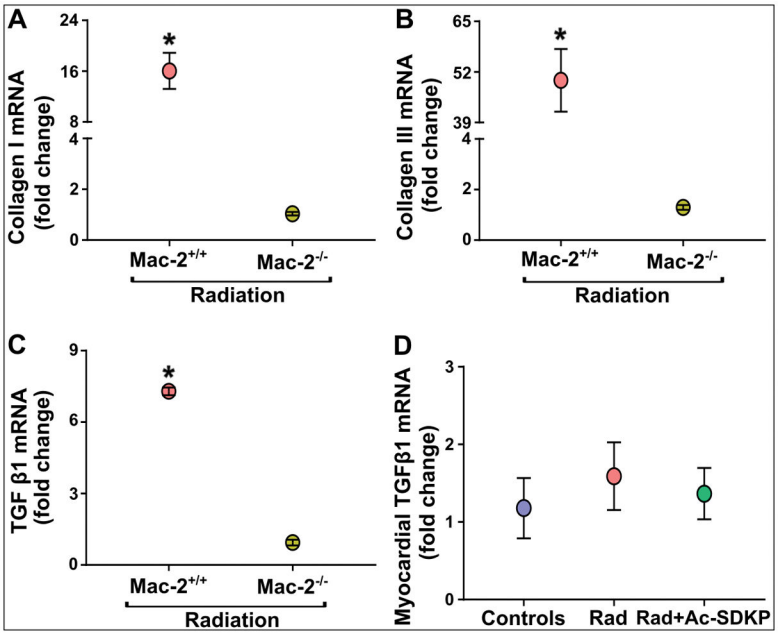

Figure 8. Quantitative *in vitro* PCR data comparing early pro-fibrotic effects of radiation in cardiac fibroblasts, and late *in vivo* TGFβ1 mRNA expression in rat hearts

Cardiac fibroblasts isolated from adult (***WT and Mac-2 knockout***) mice were exposed to radiation (9 Gy) and incubated for 72 hours in CO2 incubator; mRNA was isolated and qPCR was performed. Radiation exposure increased collagen I (**panel A**), collagen III (**panel B**) and TGFβ1 (**panel C**) gene expression in wild type cardiac fibroblast but not in Mac-2 null cells. Data are expressed as fold change of control. N = 3 each group, presented as a pooled mean of two independent experiments performed in duplicates. *, P<0.001 wild type *vs.* KO, knock out post-radiation. **Panel D** represents chronic myocardial TGFβ1 mRNA expression levels in rat hearts upon completion of *in vivo* studies, i.e., after 18-weeks of radiation. P = not significant.